STUDY ON RESISTANT MECHANISM OF ASEISMIC COUNTERMEASURE FOR GEOSYNTHETIC-REINFORCED WALL AND LEANING TYPE RETAINING WALL

Susumu Nakajima[1], Junichi Koseki[2], Kenji Watanabe[3] and Masaru Tateyama[4]

ABSTRACT

Based on the results from 1 g shaking table model tests on retaining walls with embedded sheetpile and large diameter soil nailings which have been formerly conducted, analysis on the effects and resistant mechanisms of these aseismic countermeasures is carried out. It was found from the shaking table model tests that the sheetpile worked effectively to reduce tilting of the wall facing in case the wall was situated on horizontal subsoil, while it was not so effective in case the wall was situated on sloped subsoil. In contrast, the nailings worked effectively to improve seismic performance of the walls even though the wall was situated on the sloped subsoil. More detailed analyses were also made on the effects of the horizontal and vertical resistances mobilized by the sheetpile and those of the frictional resistances mobilized around the nailings in reducing the wall displacements.

Key words: Geogrid reinforced soil retaining walls, sheetpile, nailing, residual displacements, shaking table model tests.

1. INTRODUCTION

Case histories of recent large earthquakes have revealed higher seismic performance of geosynthetics reinforced soil retaining walls (GRS walls) with full height rigid facing than conventional concrete retaining walls (*i.e.* gravity type, leaning type and cantilever type) without any aseismic countermeasures (*e.g.* Tatsuoka *et al.*, 1998; Koseki *et al.,* 2008). Based on a series of shaking table model test results which was conducted so as to investigate into seismic behaviors of the GRS walls and conventional type retaining walls (Watanabe *et al.,* 2003), it was found that the GRS walls showed more ductile seismic performances than the conventional ones because tensile resistances of the geosynthetics reinforcements could be mobilized effectively with the increase of the wall displacements. In contrast, the conventional ones showed more brittle behavior because only the subsoil reactions beneath the footing resisted against the seismic loadings. Seismic behaviors of the retaining walls constructed on the sloped subsoil and their lower seismic stabilities were also highlighted through field surveys and relevant studies on the 1999 Chi-chi earthquake, Taiwan (Huang and Chen, 2004; Huang, 2005; Kato *et al.,* 2002).

Good seismic performances of GRS walls resulted into the increase of their use in Japan not only for the retaining walls but also for the hybrid structures like bridge abutments with backfill of cement-treated gravels that are reinforced with geogrids (Watanabe *et al*., 2002) as schematically shown in Fig. 1. In addition, it has been also attempted to apply the basic concepts of the GRS walls into the integral bridge abutments as shown in Fig. 2 (Aizawa *et al.*, 2007).

On the other hand, there are some cases that the GRS walls were adopted to reconstruct retaining walls that had been severely damaged by large earthquakes (Kitamoto *et al.*, 2006). As illustrated in Fig. 3, the GRS walls were used to reconstruct and strengthen railway embankments damaged by the 2004 Niigataken-Chuetsu earthquake. Earth anchors were also installed at the toe of the walls so as to stabilize the foundation ground beneath the GRS walls, because these walls were constructed on a steep slope.

As reviewed above, there seems to be trends that the concepts of geosynthetics reinforced soil are widely used not only for the retaining walls but for the combined structures like the bridge abutments with backfill of reinforced and cement-treated gravels and the integral type bridge abutments with reinforced backfill.

From another point of view, the levels of the required performances of the GRS structures should be raised when they are applied to construct important permanent structures or to reconstruct the damaged earth structures due to the large earthquakes.

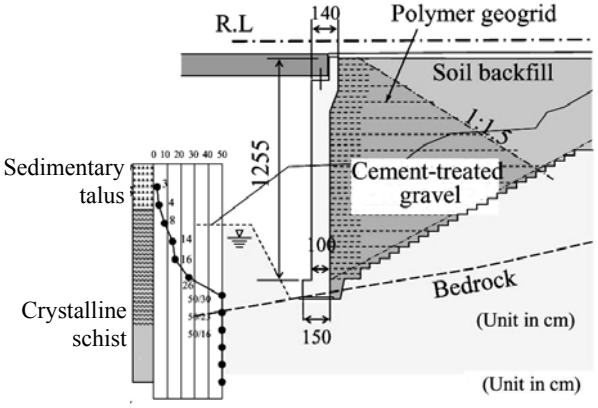

Fig. 1 Bridge abutment with cement treated gravels reinforced with geogrids (Watanabe *et al.,* 2002)

Manuscript received July 28, 2008; revised November 25, 2008; accepted November 26, 2008.

[1] Researcher (corresponding author), Public Works Research Institute, 1-6, Minamihara, Tsukuba, Ibaraki, Japan (e-mail: s-nakaji55@ pwri.go.jp).
[2] Professor, Institute of Industrial Science, University of Tokyo, Japan.
[3] Assistant Senior Researcher, Railway Technical Research Institute, Japan.
[4] Director, Railway Technical Research Institute, Japan.

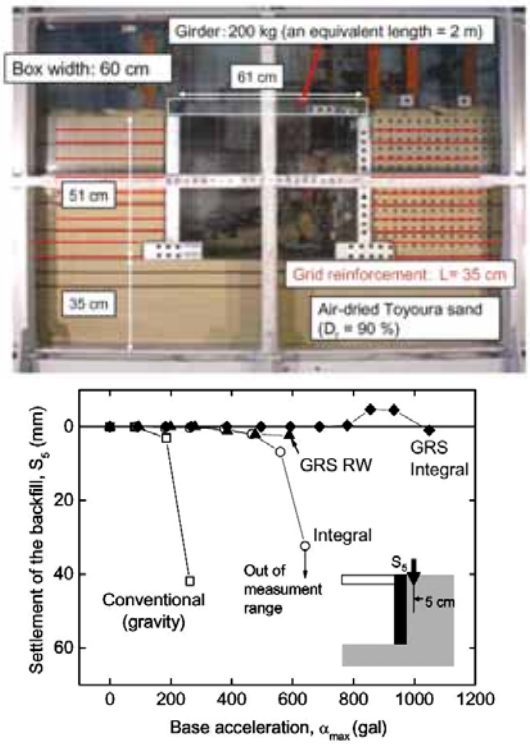

Fig. 2 Integral bridge abutments reinforced with geogrid (Aizawa *et al.*, 2007)

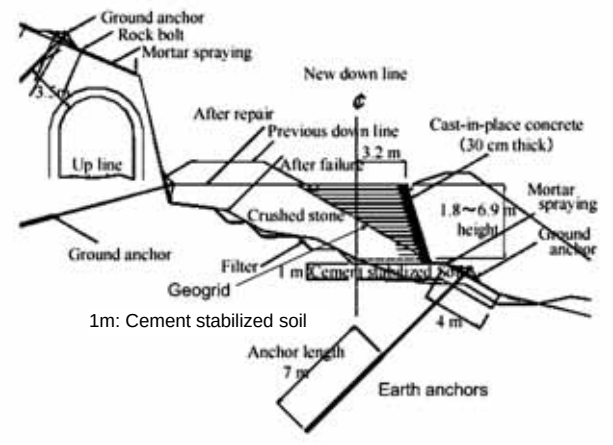

Fig. 3 Applications of reinforced soil retaining walls to reconstruction work (Kitamoto *et al.*, 2006)

In addition, it should be noted that the design seismic loads themselves in Japan have been increased. Therefore, in order to highlight the ductile seismic performance of the GRS structures especially under high seismic loading, there is a strong demand to shift the seismic design procedures of the GRS walls from specification-based design to performance-based design. In the conventional pseudo-static limit-equilibrium approach that is frequently adopted in the specification-based design, such ductile performance can not be taken into account properly.

Based on the above background, the authors have proposed the use of the sheetpile as an aseismic countermeasure for the retaining walls (Nakajima *et al.*, 2006). In this study, based on the results from a series of the shaking table model tests, the seismic behaviors of the geogrid reinforced soil retaining walls with embedded sheetpile were investigated. In addition, results from the shaking table model test on retaining walls reinforced with large diameter soil nailings (LDNs), which are currently used as an aseismic countermeasure for railway structures in Japan, were also analyzed in particular to improve seismic performances of the walls situated on sloped subsoil.

2. MODEL TEST PROCEDURES

2.1 Shaking Table and Model Retaining Walls

The model tests were conducted by using a shaking table at the Railway Technical Research Institute, Japan. The size of soil container was 260 cm long, 60 cm wide and 140 cm high. Two different types of retaining wall models were used in this study as schematically shown in Figs. 4 and 5. The center of gravity of each retaining wall is also indicated in Fig. 5. The geometric similitude for these model walls was basically set by referring to typical retaining walls having a height of about 5 m in Japan, while reducing their size to a scale of almost one-tenth.

Natural frequencies of the model retaining walls under small amplitude excitations (around 300 gals) were about 20 Hz, which were high enough as compared to the predominant frequency of the shaking motion (about 5 Hz). Thus, resonance of the model wall was not observed throughout the tests. This test condition would correspond with the actual case histories where no damage to retaining walls due to the resonance effect has been reported.

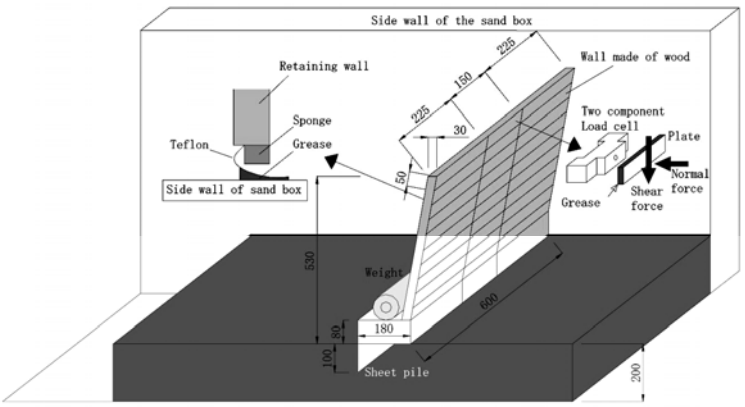

Fig. 4 Schematic illustration of model retaining wall (unit in mm)

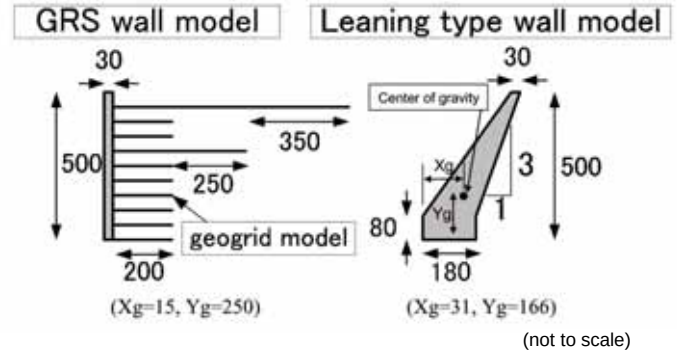

Fig. 5 Cross section of model retaining wall (unit in mm)

After the model retaining wall was placed on a subsoil layer, a backfill layer was prepared. The thickness of the subsoil was determined so that the rigid bottom platen of the soil container would not restrict the formation of the failure plane due to the bearing capacity failure. In the test SLeN (for test name, please refer to Table 1), the thickness of the subsoil was increased up to 50 cm because the failure plane in the subsoil was expected to pass deeper part than the other cases. Above the backfill layer, a surcharge of 1 kPa was applied by placing lead shots. Therefore, the effects of the horizontal inertia force induced by the surcharge were included in the measurements. Both the subsoil and backfill layers consisted of air-dried Toyoura sand (D_{50} = 0.23 mm, G_s = 2.648, e_{max} = 0.977, and e_{min} = 0.609) which were prepared by air pluviation using a sand hopper while their target relative density was set equal to 90%. This dense model ground corresponded to well-compacted sand or gravel used for actual construction of railway or road embankments which were supported by the retaining walls. It should be noted that the present model test results are affected by the boundary conditions, in particular in terms of the response of the backfill soil layer near the rigid wall of the soil container. However, due to the limitations of the available test equipment, the current dimension of the model walls and the boundary conditions were adapted in the present study, where under otherwise the same conditions, effects of the aseismic countermeasure were discussed.

Test conditions of the models to be analyzed in this study are summarized in Table 1 and Fig. 6. As summarized in Table 1, test results on the retaining walls without any aseismic countermeasures, which were previously conducted by Watanabe *et al.* (2003) and Kato *et al.* (2002), will be also referred to in this study. The case name defined in Table 1 will be used for each of the model tests hereafter. The detailed explanations on the model test preparation except for the aseismic countermeasures are described by Watanabe *et al* (2003).

Table 1 Summary of model tests conditions

Case name	Type of wall	Subsoil conditions (shape/thickness)	Aseismic countermeasures	References
HLe	Leaning type	Horizontal/20 cm	None	Watanabe *et al.* (2003)
HLeSP	Leaning type	Horizontal/20 cm	Sheetpile at the toe	Nakajima *et al.* (2007b)
HR	Geogrid reinforced soil	Horizontal/20 cm	None	Watanabe *et al.* (2003)
HRSP	Geogrid reinforced soil	Horizontal/20 cm	Sheetpile at the toe	Nakajima *et al.* (2007b)
SLe	Leaning type	Sloped/20 cm	None	Kato *et al.* (2002)
SLeSP	Leaning type	Sloped/20 cm	Sheetpile at the toe	Nakajima *et al.* (2007b)
SLeN	Leaning type	Sloped/50 cm	LDNs at wall facing and footing	Nakajima *et al.* (2007a)
SR	Geogrid reinforced soil	Sloped/20 cm	None	Kato *et al.* (2002)
SRN	Geogrid reinforced soil	Sloped/20 cm	LDNs at footing	Kato *et al.* (2002)

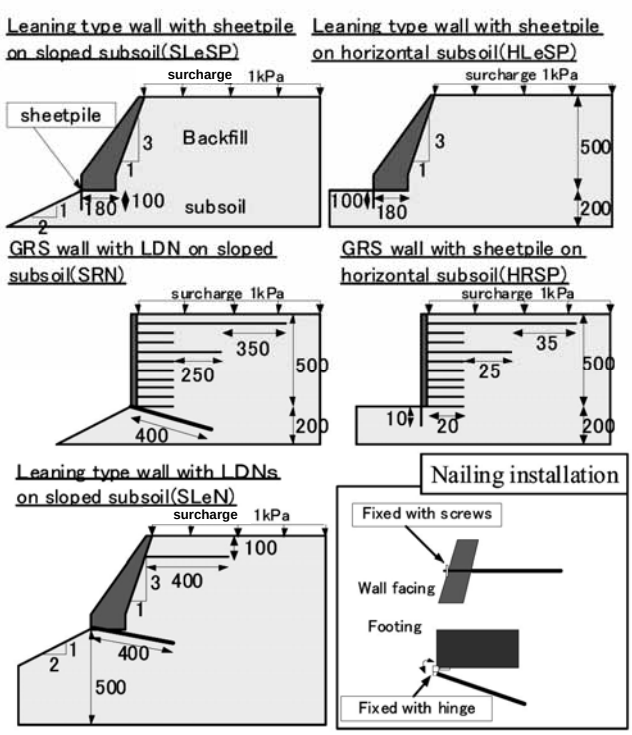

Fig. 6 Test condition of shaking table model tests (unit in mm)

2.2 Models of Sheetpile, Geogrid and Soil Nailings

As a geogrid model, phosphor bronze strips having a thickness of 0.1 mm and a width of 3 mm were prepared in a lattice shape, and their cross points were fixed with soldering as schematically illustrated in Fig. 7. These geogrid models were installed in the backfill layers at a vertical spacing of 50 mm, and they were strongly fixed with the wall facing using soldering as schematically shown in Fig. 6. Strain gages were pasted on the surface of the geogrid models so as to measure mobilized tensile resistances during the shaking, and sand particles were also glued on the surface of the geogrid models so as to mobilize their pull-out resistances effectively. As reported in Nakajima *et al*. (2008), the values of the tensile rigidity and rapture strength were 65 kN/m and 2 kN/m, respectively.

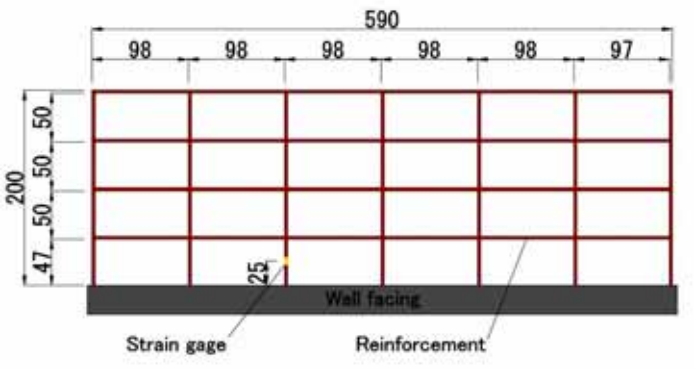

Fig. 7 Geogrid models (unit in mm)

A sheetpile model having an embedded depth of 10 cm, which was made of a phosphor bronze plate having a thickness of 0.7 mm, was fixed with a two-component loadcell which was installed at the toe of the retaining walls as schematically shown in Fig. 8. Strain gages were pasted on the surface of the sheetpile model so as to measure the bending moments during shaking. The ratio of the flexural rigidity of the model sheetpile in the prototype scale to the sheetpile (Type-III), which is used in practice, was about 1%. In this study, the flexural rigidity of the sheetpile model was reduced so as to measure the bending moment of the sheetpile easily during the shaking.

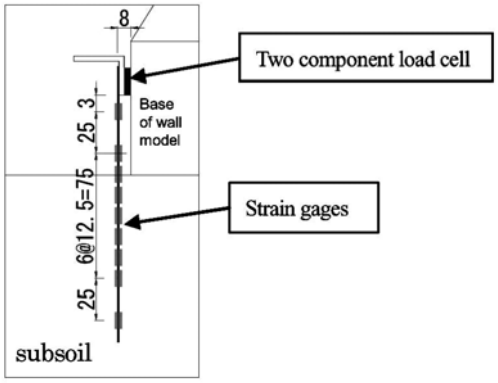

Fig. 8 Sheetpile model (unit in mm)

Model of the LDN consists of a column of improved soil and a tension bar that is located at the center of the column. Cement-treated sand and phosphor bronze bar having a thickness of 0.8 mm and a width of 5 mm were used to model the cement-treated soil column and the tension bar of the LDN, respectively. Strain gages were pasted on the surface of the improved columns so as to measure the mobilized resistances during the shaking. Top nailings were fixed with the wall facing tightly using screws, while the bottom nailings were connected with the bottom of the footing using the hinged connections so as not tot restrict the rotation of the wall as schematically shown in Fig. 6. They were prepared in advance at the specified positions before the preparation of the backfill and subsoil layers using the air pluviation technique, and thus the insertion process of these nailings was not simulated in the present study.

The geometric similitude for the models of sheetpile, geogrid and nailing was also set equal to one-tenth in this study so as to set the same value with the retaining wall model, while note that the difference in the strength and rigidity between the models and prototype ones was not considered except for the sheetpile model because the internal stabilities of these aseismic countermeasures were out of scope in this study. Further investigations are required on the effects of the similitude on these properties by referring to Iai (1989).

2.3 Seismic Loading

Seismic loading was applied by shaking the soil container horizontally using an irregular wave having a predominant frequency of about 5 Hz as typically shown in Fig. 9, while the maximum acceleration was gradually increased at an increment of about 100 gals until the wall deformed largely.

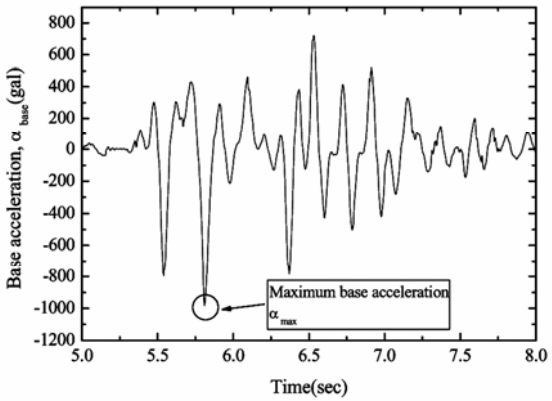

Fig. 9 Typical time history of irregular excitations

3. MODEL TEST RESULTS

3.1 Residual Displacements

Sums of residual wall displacements after the each shaking step are plotted versus the maximum base accelerations in Figs. 10 and 11. The horizontal wall displacements at the top and bottom of the wall were measured using displacement transducers. Sliding displacement at the base of the wall and tilting angle of the wall facing are highlighted in these figures as representative residual displacements and vertical arrows in the figures indicate the shaking step at which the failure plane was formed in the backfill layers. In the series of the model tests on the GRS walls, the effects of wall facing deformation such as bulging can be neglected because a full height of rigid facing was used as a wall facing, while its effects will be significant in the segmental GRS walls. Therefore, the effects of the aseismic countermeasures discussed in this study should be further investigated in the case they were applied to the segmental GRS walls.

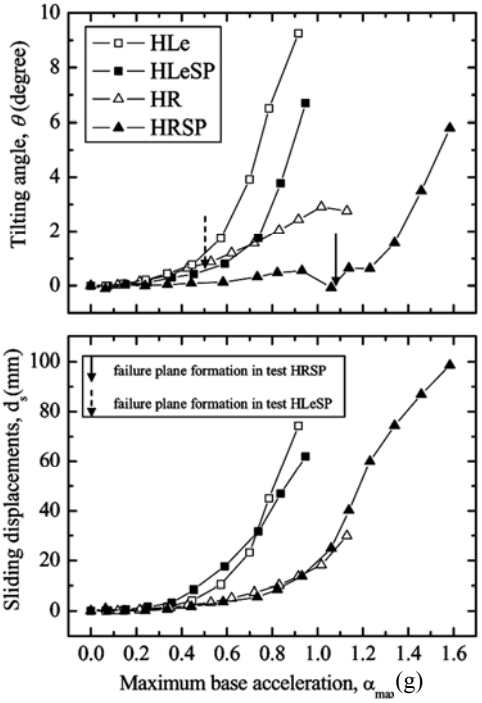

Fig. 10 Relationship between residual displacements and the maximum base accelerations (horizontal subsoil)

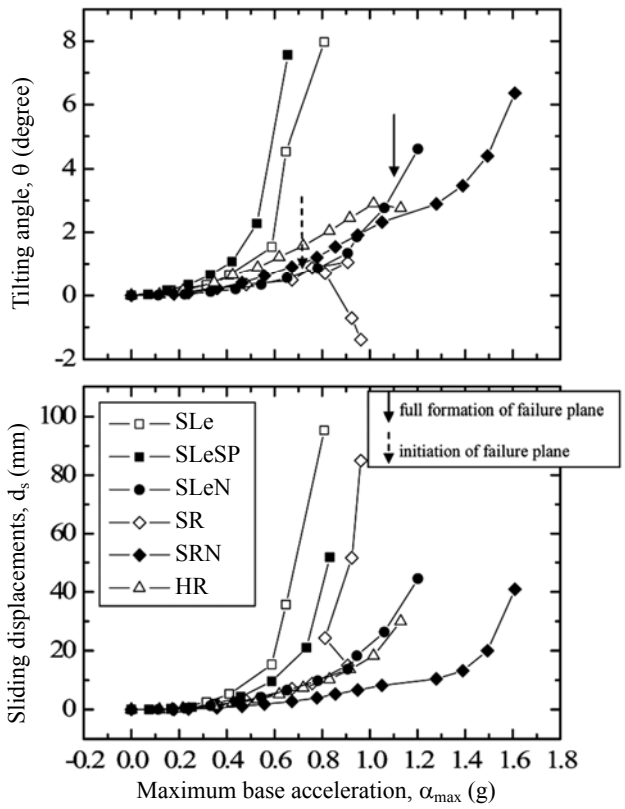

Fig. 11 Relationship between residual displacements and the maximum base accelerations (sloped subsoil)

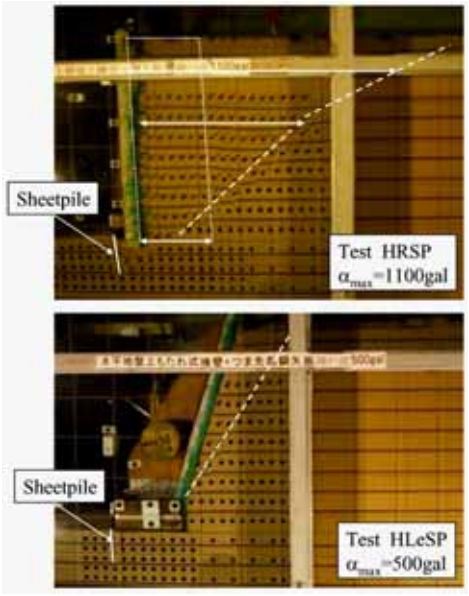

Fig. 12 Failure plane formation in backfill layer (HRSP and HLeSP)

It should be emphasized before the following discussions that the aseismic countermeasures can resist against the seismic loading under the same resistant mechanisms even if a shaking having different frequencies would be applied to the model. Because the failure patterns of the model retaining wall will not be affected by the predominant frequency of the shaking, while the amplitude of the displacements will be highly dependent on the predominant frequency of the shaking as reported in Watanabe (2007).

First, model test results on the retaining walls situated on the horizontal subsoil layers are summarized herein. As shown in Fig. 10, the GRS wall (test HR) showed much higher seismic performances than the conventional leaning type retaining wall (test HLe).

It should be also emphasized that the wall displacements increased rapidly after the failure plane formation in the backfill layer in case of the test HLe although the degrees of such accumulation was rather gentle in case of the test HR. This behavior corresponded to the observations that the failure plane initiated from the heel of the retaining walls reached to the surface of the backfill layers in a moment in case of test HLe although the development of the failure plane was restrained by the extended geogrid reinforcements installed at the middle and top of the backfill layers in case of the test HR. Similar tendencies to the test HR and HLe could be observed in the tests HRSP and HLeSP (Fig. 12).

Effects of the sheetpile as an aseismic countermeasure can be also clarified from Fig. 10. Tilting angles of the model walls with embedded sheetpile (tests HLeSP and HRSP) were smaller than those of the cases without sheetpile (tests HLe and HR) although the sliding displacements were almost equal to each other. Reduction of the tilting angle as the effects of the sheetpile was more significant in the test HRSP than in the test HLeSP. In the test HRSP, the effect of the sheetpile in reducing the tilting angle of the wall could be observed more significantly than the other cases. As shown in Fig. 10, the tilting angle of the wall facing in the test HR reached to 3 degrees at the end of the shaking of 1 g, while it could be reduced to less than 1 degree in the test HRSP. As also shown in Fig. 10, the increments of the wall displacements were accumulated even in the case of the test HRSP when the failure plane was formed at just outside of the uppermost reinforcement in the unreinforced backfill as shown in Fig. 12.

Second, model test results on the walls situated on the sloped subsoil layer are discussed herein. Accumulations of the wall displacements with the increase of the maximum base acceleration are shown in Fig. 11. Results from the test HR are also plotted in Fig. 11 for reference. It should be noted that drastic accumulations of the wall displacements were observed in the test SR even though such tendencies were never observed in the test HR. This behavior can be related with the observations that the formation of the failure plane passing through the backfill and the sloped subsoil layer, which indicates the loss of the total external stability, was observed in the test SR although such failure plane was not formed in case of the test HR.

It can be also clarified from Fig. 11 that installations of the LDNs at the toe of the retaining wall (test SRN) could effectively improve the seismic performance of the GRS walls situated on the sloped subsoil because the failure plane passing through the subsoil and backfill were interrupted by the LDNs and bearing capacity failure, which would cause the catastrophic failure of the retaining wall, was also restricted. Effects of the LDNs on the leaning type retaining walls situated on the sloped subsoil layers (SLeN) and an attempt to develop a procedure to evaluate seismic induced residual displacements based on the Newmark's sliding block analogy (Newmark, 1965) are discussed in Nakajima *et al*. (2007a).

In contrast to the effectiveness of the LDNs (tests SRN and SLeN), installations of the sheetpile could not work effectively

with the wall situated on the sloped subsoil layers (test SLeSP) because the embedment of the sheetpile could not restrict the occurrence of the bearing capacity failure.

Based on the shaking table model tests results, it was found that the embedment of the sheetpile was effective in reducing the tilting angle of the wall facing in case the wall was situated on the horizontal subsoil, while it was not so effective for the walls situated on the sloped subsoil possibly because of its lower bearing capacity. In contrast, installations of the LDNs could improve seismic performance of the wall situated on the sloped subsoil.

3.2 Resistant Mechanisms against Wall Sliding

Resistant mechanisms of the two aseismic countermeasures are investigated hereafter. Each component of horizontal resistances F_R against the wall sliding and overturning, which were mobilized by the aseismic countermeasures, is compared in the following analysis. As the components of the horizontal resistances, passive earth pressures acting on the sheetpile, horizontal component of the frictional resistances mobilized around the surface of the LDNs and pullout resistances of the geogrid models are highlighted as schematically shown in Fig. 13.

Measured resistances against the wall sliding F_R mobilized by the sheetpile and geogrid reinforcements at the timing of the maximum base acceleration in case the walls were placed on the horizontal subsoil layer are plotted versus the sliding displacement in Fig. 14. The observed timings of the failure plane formation are also indicated in Fig. 14. The values of the F_R mobilized by the geogrid reinforcements (tests HRSP and HR) were sums of the tensile forces measured by the strain gages which were pasted on the geogrid models. The value of the F_R mobilized by the sheetpile was measured by the two-component load cell installed at the fixed point between the sheetpile and wall facing as schematically shown in Fig. 8.

It can be seen from Fig. 14 that the mobilized resistances by the sheetpile (tests HRSP and HLeSP) increased with the increase of the sliding displacements while the value of F_R in the test HLeSP started to decrease with the formation of the passive failure plane in front of the sheetpile as shown in Fig. 12. Such reduction was not observed in case of the test HRSP even though larger resistance than the one in the test HLeSP was mobilized especially after the formation of the failure plane in the backfill layer with the reduction of the value of F_R mobilized by the geogrid reinforcements.

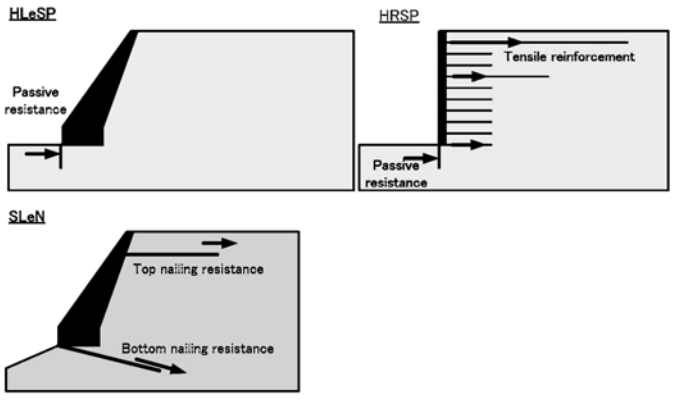

Fig. 13 Schematic diagrams of mobilized resistances against wall sliding

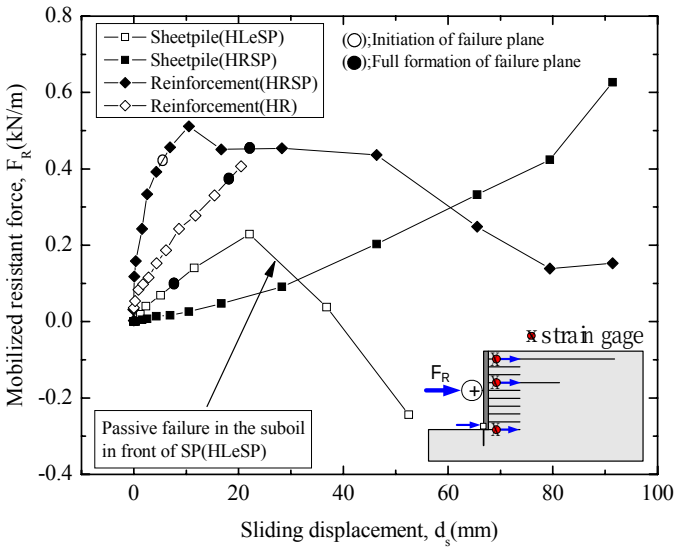

Fig. 14 Relationship between mobilized resistances and sliding displacements (horizontal subsoil)

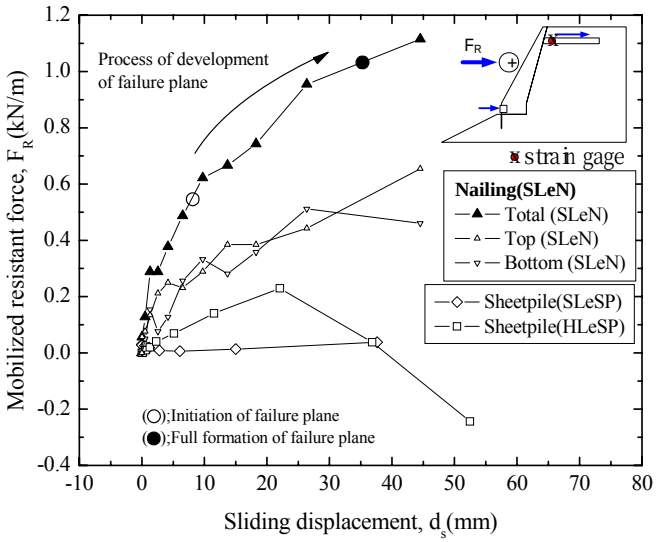

Fig. 15 Relationship between mobilized resistances and sliding displacements (sloped subsoil)

The changes of the mobilized resistance by the LDNs and sheetpile with the increase of the sliding displacement are summarized in Fig. 15. For reference, mobilized resistances by the sheetpile obtained from the test HLeSP are also plotted in Fig. 15. Horizontal component of the tensile force mobilized by the top and bottom nailings and sum of them are plotted as the mobilized resistance against the wall sliding by the LDNs. As clearly shown in Fig. 15, the value of F_R mobilized by the sheetpile in the test SLeSP did not increase during the whole shaking steps although the horizontal resistance was mobilized up to certain extents in case of the test HLeSP.

In contrast with the test SLeSP, the value of the F_R by both top and bottom nailings increased continuously during the whole shaking steps. As a result, total mobilized resistances by the LDN (*i.e.* sum of the F_R by the top and bottom nailings) increased with the increase of the wall sliding especially during the process of the failure plane formation as indicated in Fig. 15.

It was found from the above analysis that the passive resistances mobilized by the sheetpile and the frictional resistances mobilized by the LDNs resisted against the wall sliding. However, the former effect was not mobilized effectively in the cases where the passive failure of the subsoil in front of the sheetpile and bearing capacity failure of the sloped subsoil occurred.

3.3 Resistant Mechanisms against Overturning of Wall

Resistant mechanisms against the overturning of the walls reinforced with the aseismic countermeasures are discussed herein, while following the same procedures as those employed for the analysis of the wall sliding. Resistant moment against the overturning of the wall around the heel of the retaining wall M_R will be highlighted in the following analysis as schematically shown in Fig. 16.

The values of M_R mobilized by the sheetpile, nailing, and geogrid reinforcements at the timing of the maximum base acceleration are plotted versus the tilting angle of the wall in Figs. 17 and 18. Mobilized resistance by the sheetpile, called as M_{RSP}, is the sum of the resistant moment induced by the horizontal and vertical resistances acting on the sheetpile where the former component will be called as $M_{R(PSP)}$ and the latter one will be called as $M_{R(VSP)}$ in the following discussions. They were computed by considering the equilibriums of the force and moment acting on the sheetpile based on the measurement by the strain gages and the two-component loadcell as also schematically shown in Fig. 16. The values of M_R induced by the top nailing and reinforcement were also evaluated based on tensile resistance acting on them. The effect of the bottom nailing was not taken into account because it was fixed with the footing by hinges, as indicated in Fig. 16. Equations to obtain M_R are also shown in Fig. 16.

As shown in Fig. 17, the value of M_R mobilized by the reinforcement in test HRSP was larger than those in the other tests. This behavior corresponded well with the test results that the tilting angle of the wall in test HRSP could be effectively reduced. Changes of the mobilized resistance by the reinforcements in the test HRSP are compared with the ones in the test HR in Fig. 19. These values were recorded at the horizontal distances of 25 mm from the wall facing. It was found from Fig. 19 that the increase of the M_R value by reinforcement in HRSP was partially because of the increase of the tensile force mobilized by the reinforcement at the top layer. Especially after the initiation of

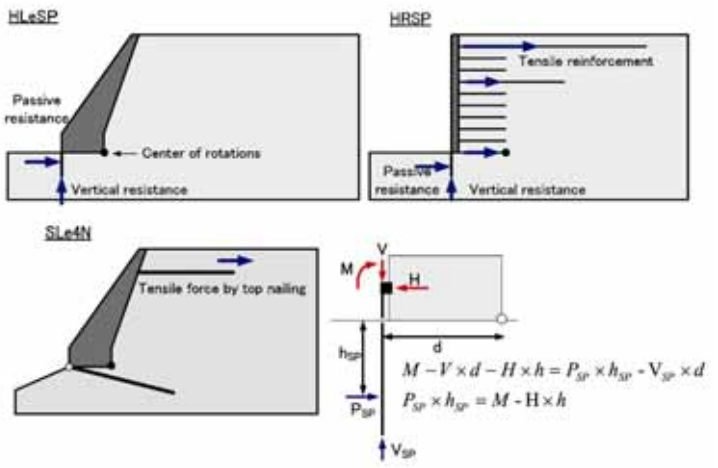

Fig. 16 Schematic diagrams of resistant moment against overturning of wall

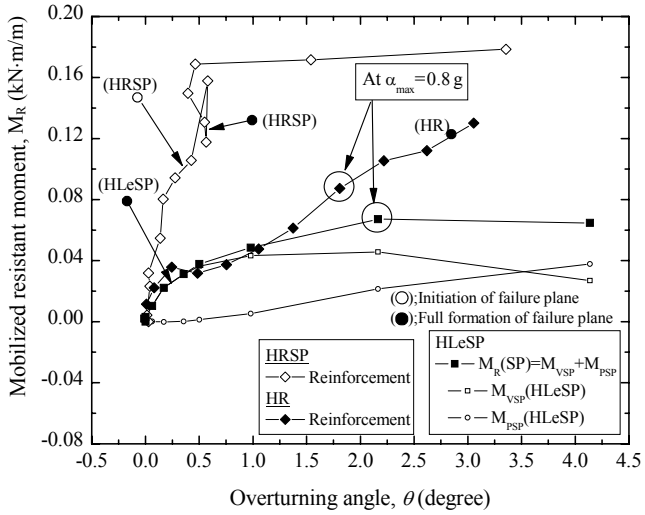

Fig. 17 Relationship between resistant moment and tilting angle of wall facing (horizontal subsoil)

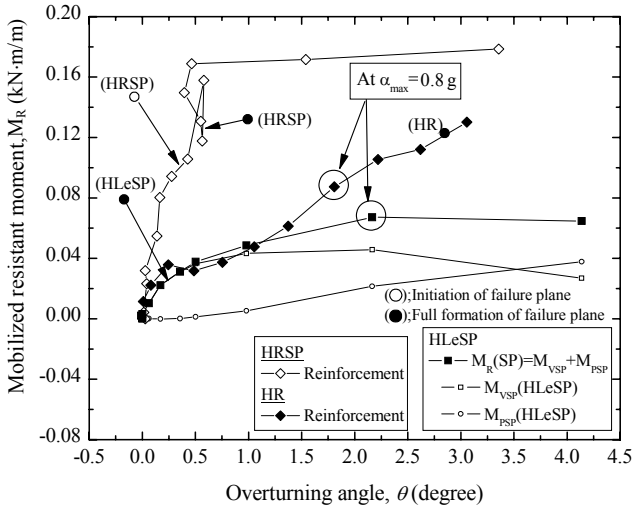

Fig. 18 Relationship between resistant moment and tilting angle of wall facing (sloped subsoil)

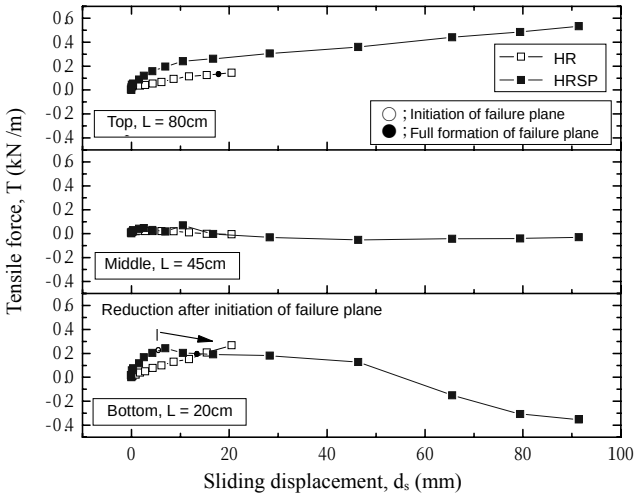

Fig. 19 Comparison of mobilized tensile force by geogrid reinforcements

failure plane formation in the backfill layers as indicated in Fig. 19, the tensile force at the top layer increased with the reduction of tensile force at the bottom layer.

As also shown in Fig. 17, the values of $M_{R(SP)}$ in test HLeSP were almost equivalent to those of M_R by the reinforcements in test HR until the maximum acceleration exceeded about 0.8 g. This behavior corresponded to the fact that the tilting angle of HLeSP could be reduced to the same extent with that of HR until α_{max} exceeded about 0.8 g.

The value of M_R by the top nailing in the test SLeN increased during the whole shaking steps as shown in Fig. 18. In contrast, the value of $M_{R(SP)}$ in test SLeSP could not be effectively mobilized. This behavior was possibly due to the low bearing capacity of the sloped subsoil, which resulted into the less mobilization of V_{SP}, which is the vertical resistance mobilized by the sheetpile as schematically illustrated in Fig. 16, and bearing capacity failure under a smaller extent of the wall tilting.

It was found from the analysis on the resistant mechanisms of the aseismic countermeasures that horizontal resistances and vertical resistances were mobilized by the sheetpile, while the latter effect was found to be effective in reducing the tilting angle of the wall. However, they were not mobilized in case the wall was situated on the sloped subsoil possibly because of the lower bearing capacity. On the other hand, the frictional resistances around the LDNs could be effectively mobilized even though the walls were situated on the sloped subsoil. It should be also emphasized that the bearing capacity failure which caused the catastrophic failure of the wall could be also restricted by the existence of the LDNs installed at the base of the wall.

It was found from the above analysis that the resistant moment was increased by the mobilizations of the vertical resistance of the sheetpile and the frictional resistances around the nailings. It should be emphasized that the negative horizontal resistances acting on the sheetpile from the backfill side toward the sheetpile, which were typically observed in the test HLeSP as shown in Fig. 14, would also increase the resistant moment against the overturning of the wall. In additions to these components which increased the resistant moment, the restraint effect of the bottom nailings on the bearing capacity failure could play an important role to reduce the tilting angle of the wall.

4. CONCLUSIONS

Based on the results from the series of shaking table model tests, seismic behaviors of the retaining walls reinforced with embedded sheetpile was investigated in this study.

1. Tilting angle of the wall facing was effectively reduced by adding the effects of the sheetpile in case the wall was situated on the horizontal subsoil. The effect was more significant with GRS walls than with leaning type retaining walls.
2. Seismic performance of retaining walls situated on the sloped subsoil layer could be effectively improved with the LDNs, while it was not the case with the sheetpile.
3. With the increase of the wall displacement, vertical and passive resistances were mobilized by the embedded sheetpile, while the former resistances worked to reduce the tilting displacement of the wall.
4. The pullout resistances around the LDNs worked effectively to reduce the wall displacement, and the formation of the failure plane in the subsoil layer could be also restricted by the existence of the LDNs.

ACKNOWREDGEMENTS

The authors wish to thank Mr. T. Sato, Research Support Promotion Member of the Institute of Industrial Science, Univ. of Tokyo, for his valuable comments in conducting all the experiments that are referred to in this paper; Mr. N. Kato, a former student of Univ. of Tokyo for his contributions in providing relevant model test data; Mr. S. Morikoshi of Integrated Geotechnology Institute Limited for his assistance in conducting the shaking table model tests.

REFERENCES

Aizawa, H., Nojiri, M., Hirakawa, D., Nishikiori, H., Tatsuoka, F., Tateyama, M. and Watanabe, K. (2007). "Validation of high seismic stability of a new type integral bridge consisting of geosynthetic-reinforced soil walls." *Proc. of 5th International Symposium on Earth Reinforcement*, Fukuoka, 819–825.

Huang, C. C. and Chen, Y. H. (2004). "Seismic stability of soil retaining walls situated on slope." *Journal of Geotechnical and Geoenvironmental Engineering*, ASCE, **130**(1), 45–57.

Huang, C. C. (2005). "Seismic displacements of soil retaining walls situated on slope." *Journal of Geotechnical and Geoenvironmental Engineering*, ASCE, **131**(9), 1108–1117.

Iai, S. (1989). "Similitude for shaking table tests on soil-structure-fluid models in 1 g gravitational field." *Soils and Foundations*, **29**(1), 105–118.

Kato, N., Huang, C. C., Tateyama, M., Watanebe, K., Tatsuoka, F. and Koseki, J. (2002). "Seismic stability of several types of retaining walls on sand slope." *Proc. 7th International Conference on Geosynthetics*, Nice, 237–240.

Kitamoto, Y., Abe, H., Shimomura, H., Morishima, H. and Taniguchi, Y. (2006). "Rapid and strengthened repair construction for a seriously damaged railway embankment during violent earthquakes." *Proc. of 8th International Conference on Geosynthetics*, Yokohama, **3**, 861–864.

Koseki, J., Watanabe, K., Tateyama, M. and Nakajima, S. (2008). "Stability of earth structures of against high seismic load." *Keynote Lecture for 13th Asian Regional Conference on Soil Mechanics and Geotechnical Engineering*, India (in print).

Nakajima, S., Koseki, J., Watanabe, K., Tateyama, M. and Kato, N. (2006), "Shaking table model tests on geogrid reinforced soil retaining wall with embedded sheet-pile." *8th International Conference on Geosynthetics*, Yokohama, **4**, 1507–1510.

Nakajima, S., Koseki, J., Watanabe, K. and Tateyama, M. (2007a). "Shaking table model tests on retaining wall reinforced with soil nailings." *5th International Conference on Earth Reinforcement*, Japan, 707–712.

Nakajima, S., Koseki, J., Watanabe, K. and Tateyama, M. (2007b). "Shaking table model tests on retaining walls with aseismic countermeasures." *13th Asian Regional Conference on Soil Mechanics and Geotechnical Engineering*, India, 613–616.

Nakajima, S., Hong, K., Mulmi, S., Koseki, J., Watanabe, K. and Tateyama, M. (2008). "Shaking table model tests on reinforced soil retaining walls by using different geo-grid models." *4th Asian Regional Conference on Geosynthetics*, Shanghai, China, 211–215.

Newmark, N. M. (1965). "Effects of earthquake on dams and embankments." *Geotechnique*, **15**(2), 139–159.

Tatsuoka, F., Koseki, J., Tateyama, M., Munuf, Y. and Horii, K. (1998). "Seismic stability against high seismic loads of geosynthetic-reinforced soil retaining structures." *Keynote Lecture for Sixth International Conference on Geosynthetics*, Atlanta, 103–142

Watanabe, K., Tateyama, M., Yonezawa, T., Aoki, H. Tatsuoka, F. and Koseki, J. (2002). "Shaking table tests on a new type bridge abutment with geogrid-reinforced cement treated backfill." *Proc. 7th International Conference on Geosynthetics, Vol.1, Geosynthetics State of the Art Recent Development,* 7, ICG-NICE, 119–122.

Watanabe, K., Munuf, Y., Koseki, J., Tateyama, M. and Kojima, K. (2003). "Behaviors of several types of model retaining walls subjected to irregular excitation." *Soils and Foundations*, **43**(5), 13–27.

Watanabe, K. (2007). *Effects of Dynamic Response of Retaining Walls and Strain Localization of Backfill Soil on Seismic Earth Pressure Under Large Earthquake Loads*. Ph.D. Dissertation, University of Tokyo (in Japanese).